

Application of transition metal ions in a study of photoinduced modifications of melanin

Andrzej Żadło✉

Department of Biophysics, Faculty of Biochemistry, Biophysics and Biotechnology, Jagiellonian University, Kraków, Poland

Short wavelength visible light is viewed as the main agent responsible for oxidative modification of melanin in the human retinal pigment epithelium (RPE). The aim of this research was to study light-induced modifications of melanin using iron and zinc as molecular probes. A synthetic model of eumelanin was treated by intense violet light. The interaction of melanin with metal ions was examined by electron paramagnetic resonance (EPR) spectroscopy and a thiocyanate assay. Weak photodegradation of melanin was shown to increase exposure of melanin subunits, while stronger photodegradation caused a loss of melanin subunits. Iron-binding in such melanin was weak and nonspecific.

Key words: melanin, oxygen, iron, zinc, transition metal ions, saturation curves

Received: 13 April, 2019; **revised:** 26 April, 2019; **accepted:** 27 April, 2019; **available on-line:** 16 May, 2019

✉e-mail: andrzej.zadlo@uj.edu.pl

Acknowledgements of Financial Support: This work was supported by the National Science Center grant (grant 2012/07/D/ST4/02211).

Abbreviations: $B_{1/2}$, half width of EPR spectrum (peak to peak distance of the first derivative); DHI, 5,6-dihydroxyindole; DHICA, 5,6-dihydroxyindole-2-carboxylic acid; DMA, synthetic eumelanin prepared by autooxidation of DOPA; DOPA, 3,4-dihydroxyphenylalanine; EPR, electron paramagnetic resonance; MDM, moderately degraded melanin; NM, non-degraded melanin; $P_{1/2}$, half power (microwave power, at which the first derivative amplitude is reduced to half of its unsaturated value); RPE, retinal pigment epithelium; WDM, weakly degraded melanin

INTRODUCTION

Melanin, one of the most ubiquitous natural pigments, is believed to play a photoprotective and antioxidant role in pigmented tissues (Meredith & Sarna, 2006; Brenner & Hearing, 2008; Kaczara *et al.*, 2012; d'Ischia *et al.*, 2015). Unlike skin melanin, melanin in human retinal pigment epithelium (RPE) shows very little, if any, metabolic turnover (Sarna, 1992). Therefore, with ageing, the RPE melanin may undergo chemical modification induced by oxygen, light and transition metal ions that are bound to melanin. The content of melanin in human RPE was shown to decrease with age (Sarna *et al.*, 2003) and the remaining melanin exhibited significant oxidative modifications that may reduce the antioxidant and photoprotective ability of melanin, and even enhance its phototoxic potential (Rózanowska *et al.*, 2002; Rózanowski *et al.*, 2008; Ito *et al.*, 2013). Light-induced degradation of melanin, which is a model of photoageing, was shown to reduce its antioxidant properties and even cause the appearance of a prooxidant action (Zareba *et al.*, 2006; Zadło *et al.*, 2007; Zadło *et al.*, 2009). It is important to stress that RPE melanin accumulates transi-

tion metal ions during a lifetime. The effect of redox active transition metal ions on melanin susceptibility to oxidative modification was previously studied (Korytowski & Sarna, 1990; Zecca *et al.*, 2008; Zadło *et al.*, 2017). The aim of this research was to examine the light-induced oxidative modifications of melanin using iron and zinc as molecular probes. Water-soluble synthetic model of eumelanin prepared by DOPA autooxidation (DMA) was used in this study. This melanin was subjected to short wavelength visible light and metal ions were added after photolysis.

MATERIALS AND METHODS

Reagents. All chemicals were reagent grade or better, and were used as supplied. Water, deionized by a millipore system (Millipore S.A. 67120 Molsheim, France), and the acetate buffer prepared using this water, were additionally treated with Chelex-100 to remove traces of metal ions.

Preparation of synthetic eumelanin. Synthetic model of eumelanin (DMA) was prepared by autooxidation of DOPA (Felix *et al.*, 1978) and purified by a modified method described previously (Szewczyk *et al.*, 2016).

Photodegradation of melanin. One mg/ml DMA in water was adjusted to pH 7.4 and irradiated by 400 nm (265 mW/cm²) light originating from a 100 W diode array illuminator (High Power UV Purple LED Chip, Chanzon, China). The initial volume of melanin solution subjected to photodegradation was 17 ml, the inner diameter of the vessel was 4.7 cm and the whole surface of solution was irradiated. During degradation, the sample was gently stirred and the temperature was maintained at 4°C by re-circulating water bath model FBC 620, Fisherbrand, Fisher Scientific GmbH, Germany. Every several hours, the pH was corrected to 7.4 by addition of a NaOH solution. At selected time intervals, appropriate amount of the melanin solution was withdrawn for EPR spectroscopy and spectrophotometry. Before taking of each degraded melanin sample, the vessel with melanin was weighted and the volume was corrected by addition of water. For selected degradation degrees, greater amounts of melanin samples were taken, lyophilized and stored in the fridge for further experiments.

Electron paramagnetic resonance (EPR) spectroscopy. EPR spectroscopy was done using Bruker EMX-AA EPR spectrometer (Bruker BioSpin, Rheinstetten, Germany). This method was used either to monitor the progress of melanin degradation (Sarna *et al.*, 2003; Zadło *et al.*, 2007) or to study the interaction of melanin with oxygen and metal ions. The progress of melanin degradation was monitored at pH 0. For this purpose, 0.1 ml of DMA sample was acidified by 0.01 ml of 37% HCl,

incubated for 0.5 hour and centrifuged at $20817 \times g$ for 5 minutes. The precipitate was washed three times with 1 ml of 1 M HCl, suspended in 0.2 ml of this acid and frozen in liquid nitrogen. On the basis of EPR measurements at pH 0, melanin was classified into the following degradation degrees: non-degraded melanin (NM) – untreated melanin that was not irradiated, weakly degraded melanin (WDM) – melanin that exhibited 19% decrease in the EPR signal, and moderately degraded melanin (MDM) – melanin characterized by the EPR signal reduced by 55% in comparison with control, which corresponds to the depletion of RPE melanin occurring at the ninth decade of life (Sarna *et al.*, 2003). For these degradation degrees, the lyophilized samples were redissolved in water to concentration of 1 mg/ml and the effects of oxygen, iron and zinc were tested. For EPR measurements with iron and zinc, 0.1 ml of the sample was mixed with 0.02 ml of 0.1 M acetate buffer (pH 5), 0.01 ml of 1.7905 mM FeSO_4 in 0.1 M acetate buffer and 0.07 ml of 0.1 M $(\text{CH}_3\text{COO})_2\text{Zn}$. Such approach produced the final concentration of 0.5 mg/ml DMA, 0.089525 mM Fe (1% w/w) and 35 mM Zn. After 0.5 hour incubation, the sample was frozen. Our EPR studies showed that iron content at the level of 1% (w/w) in human RPE melanin can be reached at the sixth decade of life (not yet published). Samples without zinc were prepared similarly except for addition of $(\text{CH}_3\text{COO})_2\text{Zn}$, and in this case 0.09 ml instead of 0.02 ml of acetate buffer was added. For measurements without transition metal ions, 0.1 ml of the sample was diluted twice by acetate buffer and frozen after 0.5 hour. To check the effect of oxygen, anaerobic version of the sample without metal ions was prepared by 0.5 hour purging by argon during continuous stirring. All EPR measurements were done at the temperature of 77 K. Typical instrumental settings for measurements of degradation degree of melanin were: modulation amplitude, 0.305 mT; center field, 336.2 mT; scan range, 7 mT; scan time, 42 s; time constant, 327.7 μs , and microwave power, 32.4 μW . The effect of oxygen and metal ions was studied at similar conditions except microwave power, which was selected in the range: 0.265 μW to 33.4 mW. To elevate signal:noise ratio, 2–20 scans were averaged. The EPR signal of iron (III) bound to melanin was measured at: modulation amplitude, 0.805 mT; center field, 158.49 mT; scan range, 140 mT; scan time, 84 s; time constant, 327.7 μs and microwave power, 5.29 mW. The final EPR spectra of iron were achieved from averaging 5 scans. The EPR measurements were carried out at 77 K. The error of EPR measurements was estimated to be 10%, and therefore only greater differences were viewed as statistically significant.

Iron (III) hydrolyses above pH 2 and at this pH melanin exhibits very weak metal-binding capacity. Therefore, iron (II) was used, however, after addition to melanin it rapidly oxidized and intense EPR signal characteristic for high-spin iron (III) was registered (Fig. 2D). 25 mM Fe(II) was achieved by dissolving FeSO_4 in argon-saturated 0.1 mM H_2SO_4 . This solution was diluted to 1.7905 mM in 0.1 M acetate buffer pH 5. Solutions of iron (II) salts were used within the day of preparation.

Determination of free iron by the thiocyanate assay. Iron, that was unbound to melanin, was determined by a modified thiocyanate assay (Luke, 1966). Due to solubility of DMA, this study was limited to samples with zinc, which caused melanin aggregation. After EPR measurements, these samples were melted and centrifuged at $20871 \times g$ for 5 minutes. 0.18 ml of supernatant was mixed with 0.01 ml of 2 M HCl and 0.01 ml of

0.1 M H_2O_2 , and heated at 100°C for 15 minutes. After cooling to room temperature, 0.1 ml of 2.5 M NaSCN with 0.01 M HCl and 0.3 ml of isopropylacetone were added. The sample was shaken on Vortex shaker for 0.5 minute and centrifuged at $20871 \times g$ for 1 minute. 0.25 ml of organic fraction was collected and fresh 0.3 ml of isopropylacetone was added. After second extraction, the organic fraction was combined with the previous one and the absorbance was measured at 500 nm against isopropylacetone. To prepare the calibration curves, 0.0179 M $\text{FeNH}_4(\text{SO}_4)_2$ (1 mg Fe/ml) in 0.0887 M H_2SO_4 was diluted to 1–5 μg Fe/ml in 5 mM H_2SO_4 . 5 mM H_2SO_4 without iron was used as concentration 0. To check the effect of acetate and zinc, similar array of Fe standards was prepared in 10 mM acetate buffer with 35 mM $(\text{CH}_3\text{COO})_2\text{Zn}$. Iron determination in supernatants from melanin was based on these standards. The error of thiocyanate assay was estimated to be 0.1 μg Fe/ml, and therefore only greater differences were viewed as statistically significant.

Data analysis. The half width ($B_{1/2}$) of EPR spectrum of melanin was measured manually. To minimize the effect of microwave power saturation, $B_{1/2}$ was determined for the minimum microwave power, i.e. 0.265 μW . The EPR spectra of NM and MDM are presented in Fig. 1A–H. If signal:noise ratio was greater than 20, the EPR signal amplitude was determined digitally, otherwise it was determined manually. The EPR signal amplitude was plotted against the square root of microwave power and the half power ($P_{1/2}$) was determined by three different approaches. The first approach, presented in Fig. 1 I–L, was that the plot was fitted with a two component function: $f(x) = A_1 \cdot x \cdot [1 + (2^{1/\varepsilon_1} - 1) \cdot x^2 / P_{1/21}]^{-\varepsilon_1} + A_2 \cdot x \cdot [1 + (2^{1/\varepsilon_2} - 1) \cdot x^2 / P_{1/22}]^{-\varepsilon_2}$ (Altenbach *et al.*, 1994), where x is a square root of microwave power, $f(x)$ is EPR signal amplitude, A_1 , A_2 are initial slopes of these two components, ε_1 , ε_2 are homogeneity coefficients and $P_{1/21}$, $P_{1/22}$ are half powers of these two components. The resulting $P_{1/2}$ was found as the value of the microwave power, at which $f(x) = 1/2 \cdot (A_1 + A_2) \cdot x$. Due to extremely high error of $P_{1/21}$ and thus of resulting $P_{1/2}$, fit of the two component function was rather qualitative than quantitative, and enabled to estimate the shape of saturation curves presented in Fig. 1I–L. The only reliable values were $P_{1/22}$ for samples with iron, which are presented in Fig. 2C. In the second and third approach, a one component function, $f(x) = A \cdot x \cdot [1 + (2^{1/\varepsilon} - 1) \cdot x^2 / P_{1/2}]^{-\varepsilon}$, was fitted in the limited range, as presented in Fig. 1M–P. In the second approach, $P_{1/2}$ was taken directly from the fitted function, while in the third approach, an additional linear function, $g(x) = a \cdot x$ was fitted to the initial five points and $P_{1/2}$ was found as the value of the microwave power, at which $f(x) = 1/2 \cdot g(x)$. For samples without iron (Fig. 1M, N), $P_{1/2}$ was determined with very high precision from the fitted function. Moreover, the EPR signal of such samples was saturated even at low values of the microwave power. Therefore, the second approach was appropriate for these samples. On the other hand, for samples with iron (Fig. 1O, P), the error of $P_{1/2}$ from the fitted equation was very high and so the third approach was applied for samples with iron.

RESULTS AND DISCUSSION

Although oxygen is paramagnetic, it had no significant effect on the general shape (Fig. 1A, B, E, F) or $B_{1/2}$ (Fig. 2A) of the melanin EPR signal registered at

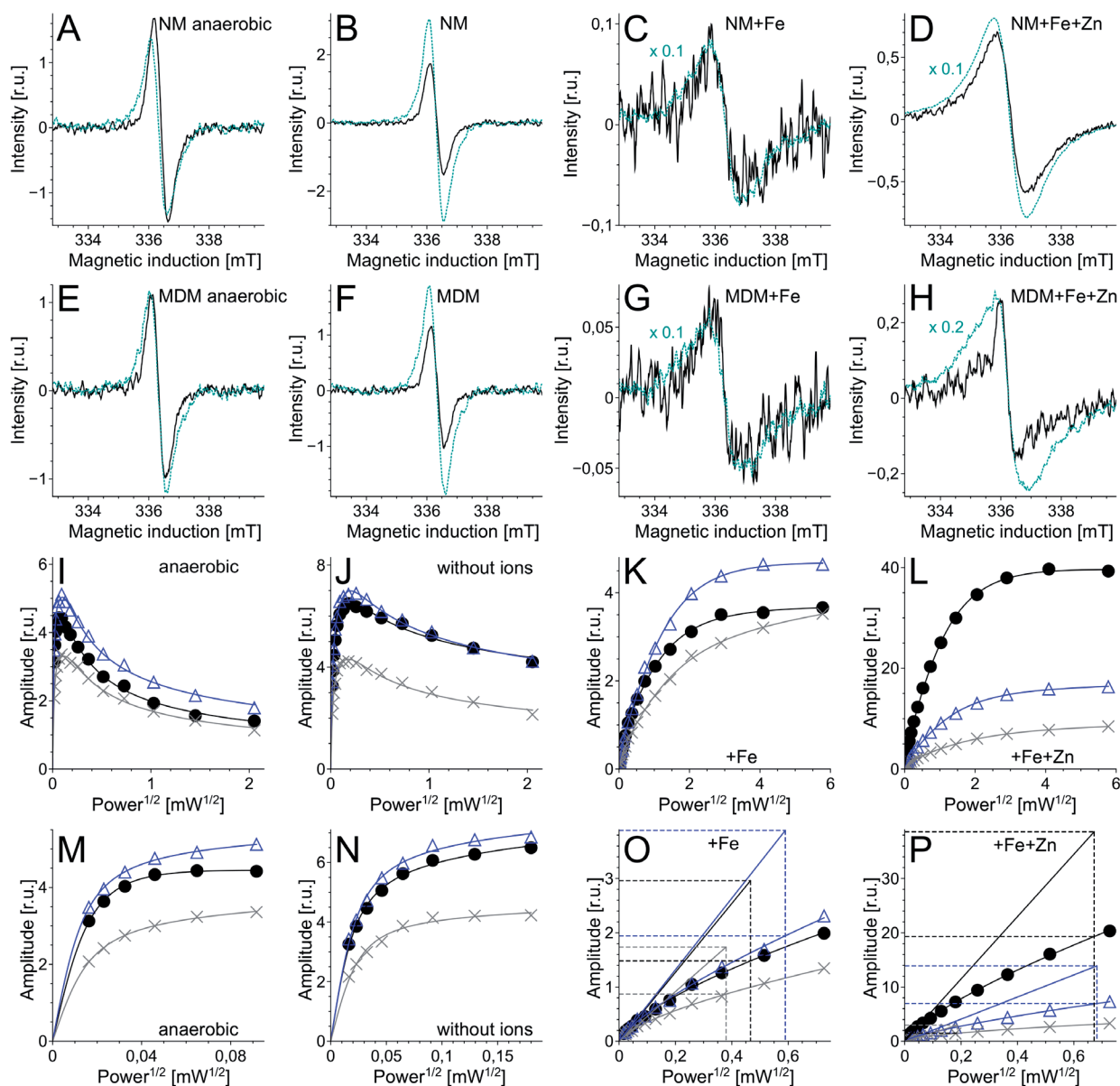


Figure 1. EPR spectra (A–H) and saturation curves (I–P) of melanin.

EPR spectra of non-degraded melanin (A–D) and moderately degraded melanin (E–H) were registered at microwave power 0.265 μW (continuous line) or 0.265 mW (dotted line). The EPR spectra of melanin with iron at 0.265 mW are multiplied by 0.1 (C, D, G) or by 0.2 (H). I–P – microwave power saturation curves of non-degraded melanin (filled circles), weakly degraded melanin (open triangles) and moderately degraded melanin (crosses). The EPR measurements were carried out under anaerobic conditions without metal ions (A, E, I, M), under aerobic conditions without metal ions (B, F, J, N), under aerobic conditions in the presence of iron (C, G, K, O) and under aerobic conditions with iron and zinc (D, H, L, P). EPR signal amplitude was plotted against square root of microwave power (I–P) and fitted with two component function (I–L) or one component function (M–P). Scale of square root of microwave power in the I–P figures represents the range of fit. The EPR measurements were carried out at 77 K.

0.265 μW . A comparison of EPR spectra registered at different microwave powers (Fig. 1A, B, E, F) and analysis of saturation curves in Fig. 1I, J reveals that the EPR signal of melanin registered under aerobic conditions saturates at higher microwave power than that registered under anaerobic conditions. $P_{1/2}$ of the EPR signal of NM in the presence of oxygen was about 1.8 times higher than that determined under anaerobic conditions (Fig. 2B), however the effect of oxygen was comparable for all studied degradation degrees. Paramagnetic iron (III) ions, that are bound by melanin, exhibit strong effect both, on the width (Fig 1C, G) and on the saturability (Fig. 1K) of the melanin EPR signal. This is because

of an efficient dipole-dipole interaction of melanin radicals with paramagnetic iron ions bound to melanin (Sarna *et al.*, 1976). $B_{1/2}$ of the EPR signal of NM with iron was about 2.9 times larger than without iron (Fig. 2A). The effect of iron on $B_{1/2}$ slightly decreased with the degradation degree, which may suggest increasing participation of modified melanin subunits that are unable to bind iron but are paramagnetic, however, photodegradation did not have a significant effect on the iron signal (Fig. 1E). The effect of iron on the saturability of melanin EPR signal was very strong. $P_{1/2}$ of NM with iron was 119 times higher than $P_{1/2}$ of such melanin without iron (Fig. 1B). Interestingly, iron increased $P_{1/2}$ of WDM

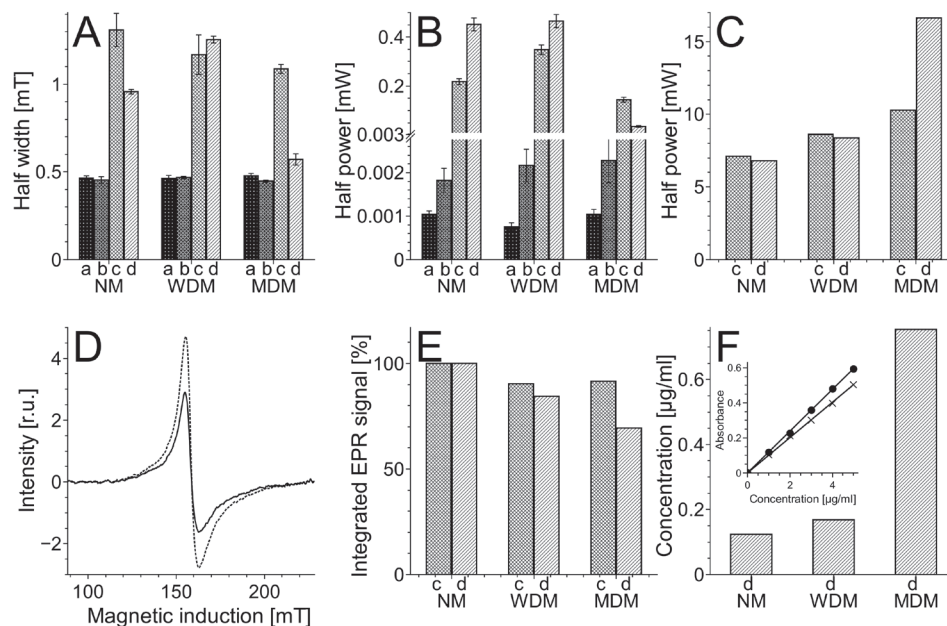


Figure 2. EPR and spectrophotometric determination of iron in melanin samples.

A – half width of melanin EPR signal registered at 0.265 μW , **B** – half power determined from one component function, **C** – half power of second component determined from two component function, **D** – EPR spectra of iron (III) bound to non-degraded melanin (dotted line) or to moderately degraded melanin (continuous line) in the presence of zinc, **E** – integrated EPR signal of iron (III) bound to melanin, **F** – iron (III) concentration in supernatant from melanin with iron and zinc. Inset in **F** – calibration curve for iron determination. The standards of iron were prepared in 5 mM H_2SO_4 (filled circles) or in 10 mM acetate buffer with 35 mM zinc acetate (crosses). Iron concentration in the samples was determined on the basis of standards in the acetate buffer with zinc acetate. NM – non-degraded melanin, WDM – weakly degraded melanin, MDM – moderately degraded melanin. The EPR measurements and iron determination were carried out under anaerobic conditions without metal ions (bar a), under aerobic conditions without metal ions (bar b), under aerobic conditions with iron (bar c) or under aerobic conditions with iron and zinc (bar d). All EPR measurements were done at 77 K.

161 times, which indicates that weak photodegradation increases exposure of melanin subunits to external factors. This increased exposure is an effect of either elevated hydrophilicity or reduced size of WDM particles (Zadło *et al.*, 2017). On the other hand, iron increased $P_{1/2}$ of MDM only by the factor of 63. This suggests that in such melanin, at least part of iron is bound by other groups than in NM. $P_{1/2}$ was increasing with the degradation degree. This suggests that this parameter can be a marker of non-degraded melanin subunits which strongly bind iron. Due to decrease in their content with increasing degradation degree, the saturation with iron of the remaining intact groups increases.

Zinc ions are another type of a molecular probe. These ions are diamagnetic and they increase the EPR signal of melanin due to stabilization of its radical form and thus shift of comproportionation equilibrium (Felix *et al.*, 1978). Indeed, the amplitude of EPR signal of NM with iron and zinc (Fig. 1D) was about 10 times higher than amplitude of NM containing only iron (Fig. 1C). On the other hand, the EPR signal of MDM with iron, measured at 0.265 μW , was increased by zinc addition only by the factor of 4 (Fig. 1G, H). This indicates that photodegradation had caused changes in the redox properties of key melanin units removing them from participation in the comproportionation equilibrium. Similar change of redox properties was previously observed for photodegraded pheomelanin (Zadło *et al.*, 2019). Interestingly, the EPR signal of MDM with iron and zinc registered at 0.265 μW was much narrower than that registered at 0.265 mW (Fig. 1H), and than the EPR signal of NM with iron and zinc (Fig. 1D). $B_{1/2}$ of such melanin was about 1.7 times narrower than $B_{1/2}$ of NM with iron and zinc, and only about 1.2 times broader than that of NM without metal ions (Fig. 2A). This indicates that in

the presence of zinc, there are some melanin subunits that are paramagnetic but they are not significantly affected by iron, which may suggest iron release. This effect is reflected in strong decrease of $P_{1/2}$ after addition of zinc to MDM with iron (Fig. 2B). Although zinc did not decrease the iron EPR signal significantly in the case of NM and WDM with iron, it decreased the EPR signal of iron bound to MDM by about 30% (Fig. 2E). Iron content in the supernatant from NM and WDM with iron and zinc did not exceed 0.17 $\mu\text{g}/\text{ml}$ (Fig. 2F), which is 0.034% (w/w), i.e. 3.4% of total iron added to melanin. On the other hand, iron content in the supernatant from MDM with iron and zinc was 0.75 $\mu\text{g}/\text{ml}$, i.e. 0.15% (w/w) or 15% of total iron added, which confirms that addition of zinc causes partial release of iron bound to MDM. This indicates that iron binding by MDM is weaker and less specific than by NM. In the NM, the iron is bound by ortho phenolic hydroxyls (Sarna *et al.*, 1981). Such groups are present in DHI and DHICA subunits. Oxidative degradation of melanin leads to destruction of DHI and DHICA subunits by ring opening and formation of carboxylic groups (Korytowski & Sarna, 1990). Therefore, it can be suggested that these carboxylic groups participate in weak and nonspecific binding of iron, which can be displaced by other metal ions. If such modifications of melanin occur in human RPE, they can increase the risk of release of iron bound during a lifetime and thus cause a prooxidant action, which could contribute to development of age-related macular degeneration.

In conclusion, weak photodegradation of melanin increases exposure of melanin subunits, while further photodegradation causes their destruction. Carboxylic groups, formed from oxidatively modified melanin subunits, can participate in binding of transition metal ions

by photodegraded melanin. Such binding is weak and nonspecific. If such modifications of melanin take place in RPE they can contribute to development of retinal pathology.

Acknowledgements

I would like to thank Sebastian Pintscher and Agnieszka Broniec for help with DMA lyophilization.

REFERENCES

- Altenbach C, Greenhalgh DA, Khorana HG, Hubbell WL (1994) A collision gradient method to determine the immersion depth of nitroxides in lipid bilayers: application to spin-labeled mutants of bacteriorhodopsin. *Proc Natl Acad Sci U S A* **91**: 1667–1671. <https://doi.org/10.1073/pnas.91.5.1667>
- Brenner M, Hearing VJ (2008) The protective role of melanin against UV damage in human skin. *Photochem Photobiol* **84**: 539–549. <https://doi.org/10.1111/j.1751-1097.2007.00226.x>
- Felix CC, Hyde JS, Sarna T, Sealy RC (1978) Interactions of melanin with metal ions. Electron spin resonance evidence for chelate complexes of metal ions with free radicals. *J Am Chem Soc* **100**: 3922–3926. <https://doi.org/10.1021/ja00480a044>
- d'Ischia M, Wakamatsu K, Cicoira F, Di Mauro E, Garcia-Borrón JC, Commo S, Galván I, Ghanem G, Kenzo K, Meredith P, Pezzella A, Santato C, Sarna T, Simon JD, Zecca L, Zucca FA, Napolitano A, Ito S (2015) Melanins and melanogenesis: from pigment cells to human health and technological applications. *Pigment Cell Melanoma Res* **28**: 520–544. <https://doi.org/10.1111/pcmr.12393>
- Ito S, Pilat A, Gerwat W, Skumatz CM, Ito M, Kiyono A, Zadło A, Nakanishi Y, Kolbe L, Burke JM, Sarna T, Wakamatsu K (2013) Photoaging of human retinal pigment epithelium is accompanied by oxidative modifications of its eumelanin. *Pigment Cell Melanoma Res* **26**: 357–366. <https://doi.org/10.1111/pcmr.12078>
- Kaczara P, Zareba M, Herrmeiter A, Skumatz CMB, Zadło A, Sarna T, Burke JM (2012) Melanosome-iron interactions within retinal pigment epithelium-derived cells. *Pigment Cell Melanoma Res* **25**: 804–814. <https://doi.org/10.1111/pcmr.12008>
- Korytowski W, Sarna T (1990) Bleaching of melanin pigments. Role of copper ions and hydrogen peroxide in autooxidation and photooxidation of synthetic dopa-melanin. *J Biol Chem* **265**: 12410–12416.
- Luke CL (1966) New spectrophotometric thiocyanate determination of iron in metals, alloys, acids and salts. *Anal Chim Acta* **36**: 122–129. [https://doi.org/10.1016/0003-2670\(66\)80013-2](https://doi.org/10.1016/0003-2670(66)80013-2)
- Meredith P, Sarna T (2006) The physical and chemical properties of eumelanin. *Pigment Cell Res* **19**: 572–594. <https://doi.org/10.1111/j.1600-0749.2006.00345.x>
- Rózanowska M, Korytowski W, Rózanowski B, Skumatz C, Boulton ME, Burke JM, Sarna T. (2002) Photoreactivity of aged human RPE melanosomes: a comparison with lipofuscin. *Invest Ophthalmol Vis Sci* **43**: 2088–2096.
- Rózanowski B, Cuenco J, Davies S, Shamsi FA, Zadło A, Dayhaw-Barker P, Rózanowska M, Sarna T, Boulton ME (2008) The phototoxicity of aged human retinal melanosomes. *Photochem Photobiol* **84**: 650–657. <https://doi.org/10.1111/j.1751-1097.2007.00259.x>
- Sarna T (1992) Properties and function of the ocular melanin—a photobiophysical view. *J Photochem Photobiol B, Biol* **12**: 215–258. [https://doi.org/10.1016/1011-1344\(92\)85027-R](https://doi.org/10.1016/1011-1344(92)85027-R)
- Sarna T, Burke JM, Korytowski W, Rózanowska M, Skumatz CMB, Zareba A, Zareba M. (2003) Loss of melanin from human RPE with aging: possible role of melanin photooxidation. *Exp Eye Res* **76**: 89–98. [https://doi.org/10.1016/S0014-4835\(02\)00247-6](https://doi.org/10.1016/S0014-4835(02)00247-6)
- Sarna T, Hyde JS, Swartz HM (1976) Ion-exchange in melanin: an electron spin resonance study with lanthanide probes. *Science (New York, N.Y.)* **192**: 1132–1134. <https://doi.org/10.1126/science.179142>
- Sarna T, Korytowski W, Pasenkiewicz-Gierula M, Gudowska E (1981) Ion-exchange studies in melanosins. In *Proceedings of the 11th International Pigment Cell Conference, Sendai, Seiji M ed.* pp 23–29. University of Tokyo Press: Tokyo
- Szewczyk G, Zadło A, Sarna M, Ito S, Wakamatsu K, Sarna T (2016) Aerobic photoreactivity of synthetic eumelanins and pheomelanins: generation of singlet oxygen and superoxide anion. *Pigment Cell Melanoma Res* **29**: 669–678. <https://doi.org/10.1111/pcmr.12514>
- Zadło A, Burke JM, Sarna T (2009) Effect of untreated and photobleached bovine RPE melanosomes on the photoinduced peroxidation of lipids. *Photochem Photobiol Sci: Official Journal of the European Photochemistry Association and the European Society for Photobiology* **8**: 830–837. <https://doi.org/10.1039/b901820d>
- Zadło A, Pilat A, Sarna M, Pawlak A, Sarna T (2017) Redox Active Transition Metal ions Make Melanin Susceptible to Chemical Degradation Induced by Organic Peroxide. *Cell Biochem Biophys* **75**: 319–333. <https://doi.org/10.1007/s12013-017-0793-6>
- Zadło A, Rozanowska MB, Burke JM, Sarna T (2007) Photobleaching of retinal pigment epithelium melanosomes reduces their ability to inhibit iron-induced peroxidation of lipids. *Pigment Cell Res* **20**: 52–60. <https://doi.org/10.1111/j.1600-0749.2006.00350.x>
- Zadło A, Szewczyk G, Sarna M, Camenisch TG, Sidabras JW, Ito S, Wakamatsu K, Sagan F, Mitoraj M, Sarna T (2019) Photobleaching of pheomelanin increases its phototoxic potential: Physicochemical studies of synthetic pheomelanin subjected to aerobic photolysis. *Pigment Cell Melanoma Res* **32**: 359–372. <https://doi.org/10.1111/pcmr.12752>
- Zareba M, Szewczyk G, Sarna T, Hong L, Simon JD, Henry MM, Burke JM (2006) Effects of photodegradation on the physical and antioxidant properties of melanosomes isolated from retinal pigment epithelium. *Photochem Photobiol* **82**: 1024–1029. PMID: 17205626
- Zecca L, Casella L, Albertini A, Bellei C, Zucca FA, Engelen M, Zadło A, Szewczyk G, Zareba M, Sarna T. 2008. Neuromelanin can protect against iron-mediated oxidative damage in system modeling iron overload of brain aging and Parkinson's disease. *J Neurochem* **106**: 1866–1875. <https://doi.org/10.1111/j.1471-4159.2008.05541.x>